

Predictive Model for the Seismic Capacity of High-Rise Building Using Deep Learning Algorithm

Rynelle Prince A. Cabauatan¹, Joshua Ericson T. Dela Peña¹, Kirk Patrick D. Doloroso^{1*}, Engr. Edgardo S. Cruz¹, Michael B. Baylon², Francis Aldrine A. Uy¹

¹ School of Civil, Environmental, and Geological Engineering
Mapúa University, Muralla St., Intramuros, Manila 1002, PHILIPPINES

² USHER Technologies Inc., Quezon City, PHILIPPINES

*Corresponding Author: kpddoloroso@mymail.mapua.edu.ph

DOI: <https://doi.org/10.30880/ijscet.2024.15.03.023>

Article Info

Received: 14 November 2024

Accepted: 20 December 2024

Available online: 31 December 2024

Keywords

Artificial intelligence, deep learning, seismic capacity, predictive model

Abstract

Seismic capacity demands continuous detailing in response to its focal function in structural health monitoring. While modern methods in engineering technology and artificial intelligence have been meeting those demands, the unpredictability of natural events, such as earthquakes, requires progressive preparations. Although instruments and models that have demonstrated their capacity to estimate structural integrity already exist, the question remains as to whether or not it produces accurate and effective real-time results. In this study, through the application of Deep Learning algorithms, an RNN-LSTM model was derived as an alternative approach to achieve more accurate predictions. Datasets collected from accelerometer sensors in two 15-storey high-rise buildings were used to measure peak ground acceleration (PGA), peak ground velocity (PGV), and peak ground displacement (PGD). The model was further validated to evaluate its capacity using performance metrics such as mean square error (MSE), mean absolute error (MAE), and root mean square error (RMSE). The produced RNN-LSTM predictive model has produced satisfactory results in comparison of the actual and predicted values as well as in the existing methods for seismic analysis. However, flaws in the approach, specifically the inadequacy of hyperparameters in sequence length, epoch, and data size, were seen as the limits of the produced model.

1. Introduction

1.1 Background of Study

Structural integrity plays a pivotal role in the life cycle of buildings and other structures. Prior to the actual construction, the design and specifications of columns, slabs, and other structural members require thorough planning and analysis. In particular, the study of Osman and Malek [1] shows that structural health monitoring (SHM) is provided to ensure the resiliency of any structure from any loads it will carry and the different circumstances it will induce through time. Although various studies have been proposed to address SHM of infrastructures, the increasing complexity, and variation of materials have affected the existing techniques and principles. In the analysis presented by AlHamayadeh and Aswad [2], damage detection remains a primary challenge for SHM due to the varying environmental conditions, such as seismic events, which alter the

structure's dynamic behavior. Furthermore, Xiong and Sheno [3] found that either fatigue or fracture causes most failures of load-carrying networks. The numerous stress cycles have led to abrupt damage in the structural material's mechanical and structural properties, which increases the dangerous risks to the structure's overall safety and serviceability. In the study conducted by Hu and Xu [4], it showed that long-period ground motions caused by large magnitude earthquakes can lead to failures on infrastructures, especially to high-rise buildings. Furthermore, the Philippines is situated within the Pacific Ring of Fire, a region where seismic and volcanic activities are most vulnerable. The Philippine fault zone has been the source of large- magnitude earthquakes for nearly two centuries, wherein it spans from the northwestern portion of Luzon to the southeastern portion of Mindanao. However, the location of the Philippine fault in Mindanao is unrecognizable due to the vegetation cover present on the island. In the northeastern region of Mindanao, where Cagayan de Oro City, Misamis Oriental is geographically located, there are four active faults nearby, namely: Cabanglasan Fault, Tagaloan River Fault, and Central Mindanao Fault lines [5]. The recent earthquake that hit the region by far was the 5.6-magnitude in Bukidnon last 2012, which placed the Cagayan de Oro City under Intensity III of the Philippine Earthquake Intensity Scale (PEIS).

Although there are instruments and models capable of recording the amount of ground movement, its accuracy remains in question whether it can provide real-time predictions over large-scale infrastructures, such as bridges and skyscrapers. For instance, the generated decision tree regression (DTR) model produced a high variance over the existing parametric models. Another system that is being employed is the time-history response model in estimating system and force parameters for the structural integrity of a building. However, this particular SHM estimation procedure does not provide accurate results, especially when input parameters are missing, as proved in the study of Jayanthan and Srinivas [6]. This limits the structure's predictive response regarding its structural health and resiliency.

Nonetheless, the timely increase in the popularity of engineering technology, such as deep learning, is leading toward a technology-based approach to civil engineering applications. Hussain et al. [7] found that the recurrent neural network (RNN) can be a viable alternative in predicting the phase angle characteristics of asphalt concrete mixtures. It was also identified that the RNN-based model, incorporated with long-short-term memory (LSTM) network, outperforms the linear regression models due to the restrictions on the variable relationship of the latter. Similarly, Zhang et al. [8] utilized a deep LSTM network to model and predict a building's structural response. However, the analysis done was solely focused on the dynamic response rather than the overall seismic capacity of buildings.

The rise of deep learning algorithms in computational analysis in the field of structural engineering has been a growing opportunity these days as they can provide a more efficient and cost-effective evaluation of structures. However, its usage has yet to be utilized fully in the country, which may eventually improve the structural health monitoring of high-rise buildings, especially under earthquake-related events.

With that being mentioned, the authors proposed to develop an efficient approach to predicting the seismic capacity of high-rise buildings using the concept of deep learning. This aims to further streamline the analysis of a high-rise building in anticipation of a major seismic event that may occur in the country anytime soon. The main objective of this research study is to establish a predictive model for determining the seismic capacity of high-rise buildings using RNN and LSTM algorithms. The following are the specific objectives:

- To collect the seismic data from the high-rise building and define the hyperparameters for the training and development of the RNN-LSTM model.
- To determine the structural behavior and performance of a high-rise building under seismic activities through understanding the effects of the seismic capacity parameters.
- To evaluate the accuracy of the RNN-LSTM model using performance metrics associated with comparing the predicted results and the actual seismic data.
- To validate the performance of the RNN-LSTM model through a comparison with the results using existing methods for evaluating the seismic capacity of high-rise building.

1.2 Literature Review

1.2.1 Seismic Capacity

Earthquakes are one of the most destructive natural disasters. In the book published by Votsi et al. [10], it is defined as the movement of discontinuities on the lithosphere's elastic portion. Based on the fault-plane diagram, as shown in Fig. 1, an earthquake begins to occur at the hypocenter, where increasing velocity underneath the earth's surface is observed. According to Kagan [11], the sudden buildup of velocity causes a sudden rupture or displacement on the ground and is transmitted to the epicenter.

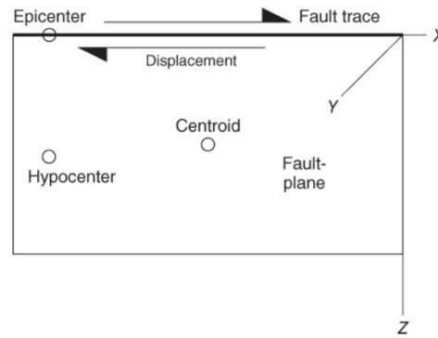


Fig. 1 Fault-plane diagram [10]

Due to the variability of the magnitude and intensity of ground shaking, earthquakes could yield extensive and prolonged implications on human life and the economy, and most notably on the infrastructures of the affected areas [12]. In addition, uncertainties continue to rise significantly regarding the vulnerability and resiliency of the built environment over such disasters [13]. Having said that, risk management and assessment should take place to thoroughly analyze the different seismic capacities of infrastructures and how they could withstand the different levels of ground motion.

In the Philippines, the Philippine Institute of Volcanology and Seismology (PHIVOLCS) is the government agency assigned to monitor seismic-related events in the country. Moreover, PHIVOLCS utilizes an Earthquake Intensity Scale, as shown in Table 1 [14], to identify the extent of damage and destruction caused by an earthquake at a certain geographic location.

Table 1 PHIVOLCS earthquake intensity scale (PEIS) [14]

Intensity	Category	PGA, g
I	Scarcely Perceptible	0.0005
II	Slightly Felt	0.0009
III	Weak	0.0011
IV	Moderately Strong	0.005
V	Strong	0.01
VI	Very Strong	0.12
VII	Destructive	0.21
VIII	Very Destructive	0.36 – 0.53
IX	Devastating	0.711 – 0.86
X	Completely Devastating	1.15<

1.2.2 Seismic Assessments of Structural Systems in the Philippines

In the Philippines, most studies conducted involving seismic analysis of buildings have utilized the nonlinear and probabilistic approaches. Peñarubia [14] found that the design philosophy used for most structures in the country is based on the base shear as derived from the design ground motion. However, he added that the recently recorded seismic events exhibited high intense acceleration values as compared to the design ground motion. This implies that the existing structures are more susceptible to damage even at low-magnitude earthquakes. Differences in the building's structural system offer varying observed behavior under the influence of seismic activities. Through elasto-plastic time-history analysis, Luo et. al. [15] uncovered those systems like frame structure, frame-shear wall structure and shear wall structure of building in the Philippines have met the requirement that beam yields first, however vertical force component does not yield. While all said systems show good seismic behavior, frame-shear wall structures are seen to provide best results. The idea was further supported by Vaisakh and Nair [16] through structural configuration testing of Braced, Rigid Frame and Frame-shear buildings. Wherein Frame-shear structural system has also shown the best performance. This indicates that while some buildings in the Philippines have already been using the best structural system for seismic activities, they are still prone to earthquakes.

1.2.3 Deep Learning Application in Civil Engineering

In the context of the advancements in the building and infrastructure industry, traditional methods for structural analysis are proving insufficient to meet the demands of the modern era, which require intelligent

synchronization and real-time simulation. This has led to the emergence of a new research field known as artificial intelligence-based computation in civil engineering. In the study conducted by Wang et al. [17], a comprehensive review of research on the application of AI technology in material and structural analyses within civil engineering was conducted. The aim was to provide an overview of the current progress in this field. The research was categorized into three main areas: static feature studies, dynamic feature studies, and composite feature studies, based on the type of problem inputs. The study delved into the general methodologies, commonly used AI models, and representative applications within each research category. Furthermore, the strengths and weaknesses of the current studies were discussed. To demonstrate the accuracy and efficiency of AI models compared to conventional numerical methods, a specific example was highlighted: an end-to-end deep learning framework for structural analysis. This example showcased the potential of AI models in achieving accurate and efficient results. Finally, the study identified four open problems from an engineering application perspective, highlighting major challenges and suggesting future research directions for AI-based computational analysis in civil engineering. By addressing these challenges, the field can continue to advance and provide innovative solutions for the industry's evolving needs.

1.2.4 Recurrent Neural Network (RNN)

Neural networks suited for time-series and sequential data are an extension of feedforward networks called Recurrent Neural Networks (RNN). According to Singh et al. [18], a distinctive feature of RNN is the ability to process variable-length sequences that focus on modelling in the temporal domain. Unlike feedforward neural networks, RNN can process data one at a time, retaining a state, or memory, that reflects an arbitrarily long context window which BIM identified as features collectively useful in ordinal and temporal problems, such as image captioning, language translations, and speech recognition. However, he claimed that though RNNs are readily efficient and accurate compared to earlier versions, it is complicated to train and often consist of millions of parameters. Like ANN and Deep Learning, RNN uses layers of data with multiple inputs, weights, and parameters to produce accurate output.

According to Kim [19], the use of recurrent neural networks (RNN) to create a simulation model for the time history response of building structures can help address exertion in computation using finite element method (FEM) even with semi-active control systems. Semi-active control devices are specialized components or systems used in structural engineering to mitigate the effects of dynamic loads, such as seismic forces, on buildings and other structures. Unlike passive control devices that operate based on fixed properties, semi-active control devices can actively adjust their characteristics to adapt to changing conditions. In his study, two examples of building structures were considered, an 11-storey building and 27-storey building both with semi-active control systems of magnetorheological dampers. The RNN model underwent training with a dataset comprising five historical earthquakes and five artificially generated ground motions. Its performance was subsequently assessed using two additional artificial ground motions and one historical earthquake, none of which were part of the training data. The outcomes demonstrated that the developed RNN model outperformed the FEM model by providing highly accurate seismic responses at the same time with reduced computational expenses.

1.2.5 Long-Short Term Memory Network (LSTM)

Similar to RNN, LSTM has recently catered to the need to predict nonlinear time-variant system dynamics. In many cases, LSTM infrastructure has been known as a classic action recognition algorithm that has become a basis for effective hybrid algorithms. Chen et al. [20] identified that LSTM has the capability to strengthen the recognition technology in differential characteristics of human action to reflect the change of speed. Time-series data used by neural networks are obtained using continuous real-valued data points taken over time. These kinds of data are used and processed by LSTM to solve complex, artificial long-time-lag tasks such as high forms of predictions.

According to Xing et al. [21], LSTM can calculate expected output, actual output, and weight matrix with minimum error through this process. Each layer of an LSTM architecture consists of memory blocks, each with components that are generally "smarter" than classical neurons. Each block operates by using gates to control where the inputs go via sigmoid activation, triggering a change of state and adding information through different conditions. The conditions that decide the output are based on the input, memory, and the three types of gates as shown in Fig. 2 [21].

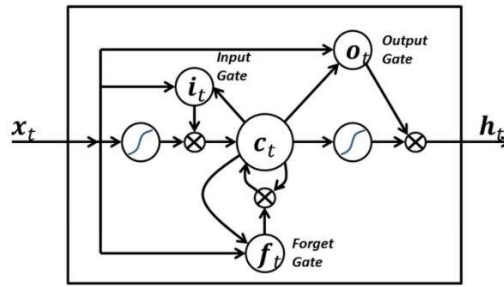


Fig. 2 Standard LSTM architecture [21]

At each time step t , during these processes, the hidden state vector h_{t-1} at time $t-1$ and the cell state vector c_t at the current state are transferred to the next time step $t+1$, wherein both will serve as the short-term and long-term memory. To address problems regarding vanishing and exploding gradients, a nonlinear function of the previous inputs and hidden states is needed. Therefore, input gates during process state monitoring and output gates can be expressed respectively as:

$$i_t = (W_{xi}x_t + W_{hi}h_{t-1} + b_i) \quad (1)$$

$$o_t = (W_{xo}x_t + W_{ho}h_{t-1} + b_o) \quad (2)$$

Where W_{xi} , W_{xo} , b_i , and b_o represent input and output weights and biases, respectively. The units corresponding to weights and biases are measured depending on the nature of the individual error. In the backward pass process, partial derivatives are used to expand the weight contribution to propagate back only to t , where the error occurred. Since LSTM networks have a fixed weight of "1", the memory cells tend to lose their memorizing capability due to the continuous stream of input variables. Forget gates are applied by replacing the weight "1" with other ranges but are still computed through a similar process or can be simply expressed as:

$$f_t = (W_{xf}x_t + W_{hf}h_{t-1} + b_f) \quad (3)$$

Where W and b are weights and biases of forget gate. In choosing desired weight and biases, the number relies on their performance obtained in cell state. In some cases, according to De la Fuente [22], weights at different gates tend to produce the same number under the event called the temporal pattern of weight distribution. This means that models with lag-memory hyperparameter values can already provide the best performance. In generating correct hyperparameters, biases and variance are needed to be considered. According to Hoque and Aljamaan [23], while in some cases, like programs under Kernel Ridge Regression, show optimal performance without hyperparameter tuning, cases of producing poor-performing models are demonstrated to be more frequent. Implying the importance of tuning and un-tuning for optimization. This was further supported by Sipper [24], through small-scale and large-scale experiments containing 28,857,600 algorithm runs. The results have shown that the large-scale investigation involving 26 Machine Learning Algorithms and 250 datasets provided a preview of how hyperparameter tuning helps maximizing the desired function and optimal performance.

1.2.6 RNN and LSTM Algorithm in Seismic Analysis

The study of Huang et al. [25] presented an approach that uses recurrent neural network (RNN) to forecast slope dynamic responses. This approach addresses the struggle to accurately forecast the dynamic behavior of complex sloping systems using the conventional method like the finite element method (FEM) which relies on simplified physical models. The authors employed three RNN models namely simple RNN, LSTM and Gru models. Moreover, a multi-layer perceptron model was trained for comparative purposes to the three RNN models. The data utilized for the training and test dataset of the models were from extensive shaking-table experiments. Three experiments were conducted to assess the impact of data volume on the models. The results demonstrate that recurrent neural networks excel in analyzing the seismic dynamic responses of slopes, surpassing the predictive accuracy of the multi-layer perceptron network. This study shows that recurrent neural networks are well-suited for time-series prediction of dynamic responses to seismic forces which has potential to contribute to the reduction of future risks associated with earthquake-induced disasters.

Furthermore, the study of Li [26] showed a framework based on deep learning techniques which is utilized for seismic structural health monitoring of structures. This framework utilizes a Long Short-Term Memory

(LSTM) Encoder-Decoder architecture, a variant of Recurrent Neural Networks (RNN), applied to time series data. The LSTM network processes the data and condenses it into a Latent Space Vector (LSV), which is then used with traditional ML algorithms to output the structural health conditions, including overall health, damage locations, and severity. The study also presents a fast prediction method using LSTM network variants and a Temporal Convolutional Network (TCN) to accurately predict the structural response for rapid decision-making.

Additionally, an Optimal Sensor Placement (OSP) method is proposed to ensure high-quality data collection, and a method to effectively collect and summarize reconnaissance results using social media posts and official resources following an earthquake event is presented. The framework is applied on a 6-story hotel in which the predicted responses are generated using the LSTM model with convolution filters. The results demonstrate a high level of correlation between the actual and predicted acceleration responses, with the two being very similar to each other. This provides an efficient and accurate method to automate and enhance the monitoring and reconnaissance processes for buildings and other civil structures.

2. Methodology

2.1 Conceptual Framework

As presented in Fig. 1 below, the structural threshold acceleration data in x, y, z-directions of two 15-storey residential high-rise buildings in Cagayan de Oro City is the primary input values for the deep learning (DL) based model, particularly Recurrent Neural Network and Long Short-Term Memory Network (RNN-LSTM). Specifically, datasets from the lower, middle, and upper floors will be fed into the RNN-LSTM model for development and training. After establishing the model, it will be validated using experimental and field data. The model's performance will be evaluated using various performance metrics as well as existing methods for structural analysis of buildings. Finally, the output of the study is the predictive model for the seismic capacity of high-rise buildings.

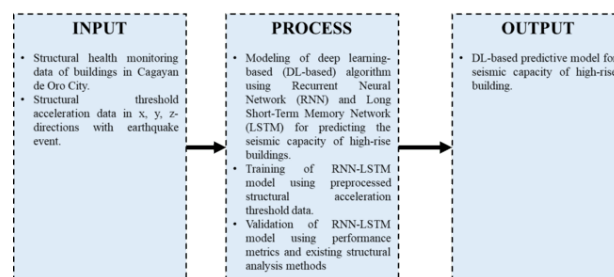


Fig. 1 Conceptual framework of the study

2.2 Data Gathering Procedure

Multiple data gathering procedures were utilized to maximize both efficiency and accuracy of the results. These were specified depending on the need of different phases based on their type, target, and requirements by the approach used.

2.2.1 Identifying Existing Risks and Challenges and Setting of Parameters

In this phase, existing local and foreign literature and studies will be considered in finding out the existing risks and challenges associated with high-rise buildings and its seismic capacity. This will be the primary basis for the identification of input parameters as to where the seismic capacity of high-rise buildings can be predicted. In addition, a background study for deep learning, specifically recurrent neural network (RNN) and long short-term memory (LSTM) network, will be performed to determine related methodologies that can be replicated in the existing study.

2.2.2 Dataset Collection and Processing

Information regarding the needed as-built structural models and sensor acceleration data of the two 15-storey residential high-rise buildings in Cagayan de Oro City will be acquired through data request made to USHER Technologies, Inc. The sensor acceleration data will be pre-processed to eliminate noise and outliers which may affect the dataset. In addition, acceleration data on x, y, and z axes will be extracted from the pre-processed data for normalization prior to model training. Meanwhile, the pre-processed data will be split into training and testing datasets which will be used for the training and evaluation of the RNN-LSTM model, respectively.

2.2.3 RNN-LSTM Model Development Using Keras API

The pre-processed and normalized experimental datasets will be stored and converted into a comma-separated values (.csv) file extension. It will then be imported to Keras sequential API, a Python-based deep learning application programming interface (API) developed by Google [27]. Using Keras sequential API, a data structure will be established through Array Data Structure. Mutable Arrays of Single Bytes shall be used so that the program can overwrite, add, or remove elements such as the byte array object. The byte array produced has the capacity to shrink, grow and be converted back into immutable bytes object. Through this process, the weight of initial inputs and the value of hidden layers will be computed to initialize RNN. The output weight will be used as initialized weight of neurons, which will undergo feature scaling and will be split for train and test in LSTM. The features (pre-processed data) will be then converted into NumPy array for reshaping based on shapes that are accepted by LSTM model. With the initialized RNN weights and created LSTM layers, the dataset will be compiled and fitted to calculate the activation function. The NumPy array will be imported to produce an output activation between 0 and 1. Finally, a program architecture will be built. Using Adam optimizer and mean square error (MSE) loss function, the initialized RNN will be made into a sequential model wherein LSTM layers with parameters will be added. The final layer or output layer, a fully connected dense layer, will be established to predict a value of seismic capacity.

2.2.4 Model Training

With the final layer or output layer for the prediction being established, the RNN sequential model, with the LSTM layers added, will then undergo model training using training dataset. Using historical and collected data to produce training and validation data, the topology and size of neural networks will be determined through this phase. The training progress will be closely monitored to re-assess and re-evaluate hyperparameters, such as epoch. Depending on the results of the next phase, Model Validation, the hyperparameters will either repeat training and go through tuning or proceed to evaluation using performance metrics. Finally, if the model has successfully undergone training, the weights of output trained model will be saved for future usage.

2.2.5 Model Validation

In this phase, the trained model will now be tested using testing dataset and performance metrics. The Processing and Review Interface for Strong Motion (PRISM) software, an earthquake engineering software, will be utilized to obtain the ground motion, response time history, and response spectra data of the buildings. To provide statistical measure as to how well the regression predictions approximate the real data points, R-square will be used as primary evaluator. Mean Square Error (MSE) will then be used to generate measures on how close the approximated regression line is to a set of data points. Through this method, the study will also be able to interpret how perfect is the generated predictive model. Mean Absolute Error (MAE) will also be used to measure the absolute difference of the actual and predicted values. Taking no considerations of their direction in the regression model. Finally, the Root Mean Square Error (RMSE) will be utilized to produce a numeric accuracy of the produce model in terms of the average difference between the values. In this phase, the generated model is tested and tuned repeatedly to obtain optimal results.

3. Results

3.1 Identifying Existing Risks and Challenges and Setting of Parameters

Considerations done with the re-assessment of published data and existing methods have resulted in the identification of input parameters as well as the correct discernment of data sets as to where seismic capacity of high-rise buildings can be predicted. With the gathered information, a derived simplified RNN-LSTM process is made for an effective modelling and deployment.

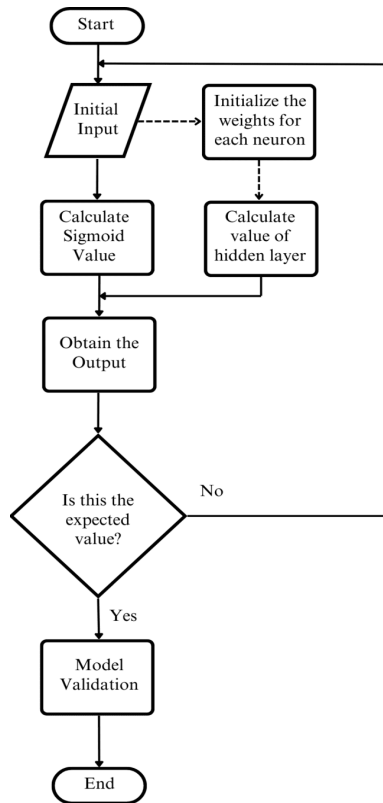


Fig. 2 Derived RNN-LSTM training process

3.2 Dataset Collection and Processing

Information regarding the gathered data of acceleration sensors positioned in the two residential high-rise buildings in Cagayan de Oro City acquired from USHER Technologies Inc. Prior to pre-processing and normalization, the descriptive statistics of the sensor acceleration data were performed as shown in Table 2. The comparatively small values are acceleration in the structure’s directions. Since the seismic activity in scale is only at an average of Intensity 1, it is expected that there is no relative rotation in the structure’s body given that a 90-degree rotation is measured at 0.5. Negative values on the other hand shows acceleration towards the opposite side of the sensors.

There is a difference in the number of recorded data for each floor wherein it can be observed that higher-level floors show greater number of acceleration data as recorded by the installed sensors. This difference is due to their location wherein higher floors are more susceptible to vibrations due to lower damping. It was found that higher floors tend to produce higher vibration frequency and greater number of occurrences [28]. The individual data on the other hand were used to identify peak ground acceleration, peak ground velocity, and spectral acceleration.

Furthermore, 67 percent or two-thirds of the total number of data are allocated as training data, while 33 percent or one-third of the total number of data is used as testing data. This splitting ratio is regarded to minimize the computing time and reduce discrepancies in the characteristics of models in Bootstrap [29].

Table 2 Statistical parameters of sensor acceleration data

Building, Floor	Variable	Mean	Max	SD
Tower 1, Lower (L/F)	X-Direction, in g	0.0000260	0.0056	0.00122
	Y-Direction, in g	0.0000329	0.0065	0.00124
	Z-Direction, in g	-0.0000040	0.0029	0.00046
	Intensity	1.1137627	2.0000	0.31753
Tower 1, Middle (M/F)	X-Direction, in g	0.0000279	0.0118	0.00294
	Y-Direction, in g	-0.0001940	0.0143	0.00293
	Z-Direction, in g	0.0000013	0.0021	0.00041
	Intensity	1.3124354	4.0000	0.46525

Tower 1, Upper (U/F)	X-Direction, in g	0.0000108	0.0177	0.00385
	Y-Direction, in g	-0.0001284	0.0221	0.00507
	Z-Direction, in g	0.0000475	0.0028	0.00043
	Intensity	1.3907005	4.0000	0.56498
Tower 3, Lower (L/F)	X-Direction, in g	0.0000298	0.0069	0.00114
	Y-Direction, in g	-0.0000863	0.0068	0.00118
	Z-Direction, in g	0.0000072	0.0025	0.00057
	Intensity	1.0921156	2.0000	0.28920
Tower 3, Middle (M/F)	X-Direction, in g	-0.0000836	0.0138	0.00253
	Y-Direction, in g	-0.0001326	0.0138	0.00275
	Z-Direction, in g	-0.0000586	0.0024	0.00040
	Intensity	1.2643939	2.0000	0.44102
Tower 3, Upper (U/F)	X-Direction, in g	-0.0000766	0.0177	0.00332
	Y-Direction, in g	-0.0002509	0.0239	0.00402
	Z-Direction, in g	0.0000262	0.0028	0.00041
	Intensity	1.3451389	4.0000	0.51610

3.3 RNN-LSTM Model Development Using Keras API

In this study, the `seq_length` and `epoch` were the two parameters considered to improve the performance of the RNN-LSTM model. Moreover, the `seq_length` was determined based on the results recorded by the accelerometer. Meanwhile, epochs of 10, 25, and 50 were utilized which signify the number of times that the entire training dataset passed through the model during training. The dataset was split into two wherein 67% of it was used as train data set and the remaining 33% was for the test data set. A `seq_length` value of 100 was used, while a dense value of 3 was used to represent the registered features X, Y and Z directions. These features are measured movements in three-dimensional directions due to the vibrations and acceleration in the structures. To ensure that the hyperparameters are set with the assigned values, a sequential API was used to manually create models layer-by-layer. In this process, the program analyzes data from top to bottom of the layers, ensuring that the datasets undergo complete fitting and evaluation before producing a single output. Specifically, the sequences made are `trainX` and `trainY` for training and `testX` and `testY`.

Table 3 Summary of weights and biases of the RNN-LSTM prediction model

Building, Floor	Weight matrix shape (W)	Recurrent weight matrix shape (U)	Bias vector shape (b)
Tower 1, Lower (G/F)	(100, 400)	(3, 400)	(400, 0)
Tower 1, Middle (M/F)	(100, 400)	(3, 400)	(400, 0)
Tower 1, Upper (U/F)	(100, 400)	(3, 400)	(400, 0)
Tower 3, Lower (G/F)	(100, 400)	(3, 400)	(400, 0)
Tower 3, Middle (M/F)	(100, 400)	(3, 400)	(400, 0)
Tower 3, Upper (U/F)	(100, 400)	(3, 400)	(400, 0)

The Table 3 shown presents the summary of weights and biases of the input and output gates of the RNN-LSTM prediction model. The values of matrix and vector shapes were similar for lower, middle, and upper floors of the two towers which signifies that the LSTM layer shares similar weights across the time steps. When incorporated to the general equation, the input gate of the RNN-LSTM prediction model is in the form of:

$$i_t = (100x_t + 3h_{t-1} + 400) \quad (4)$$

This shows that the model has 100 units in the hidden layer and each unit is connected to 400 input features. Moreover, the recurrent weight matrix shape represents that there are 3 LSTM units, where each unit has 400 connections from the previous hidden state. Similarly, the general equation of the output gate of the RNN-LSTM prediction model is expressed as:

$$o_t = (100x_t + 3h_{t-1} + 400) \tag{5}$$

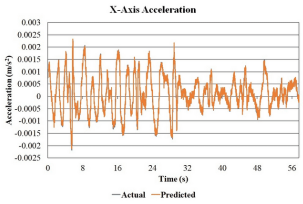
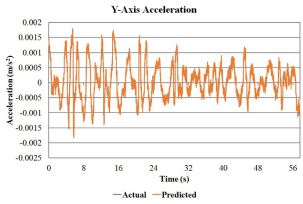
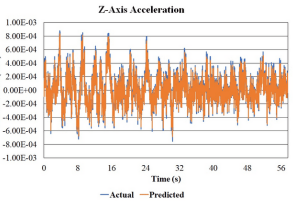
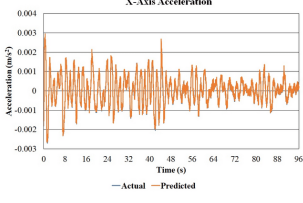
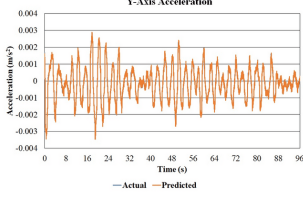
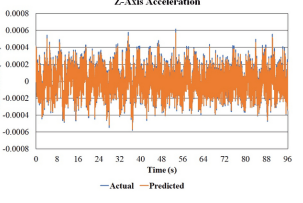
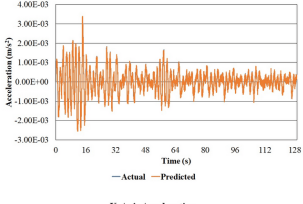
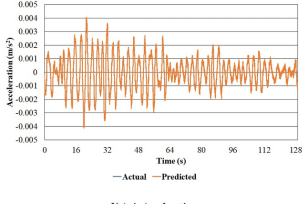
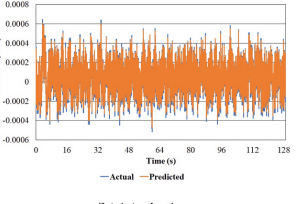
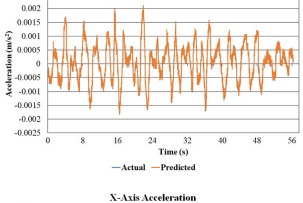
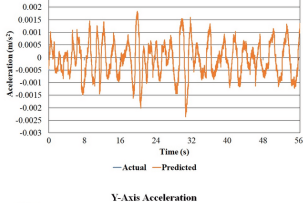
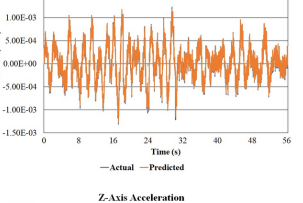
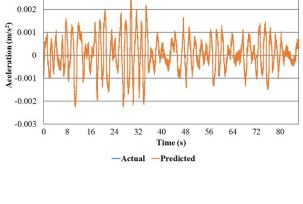
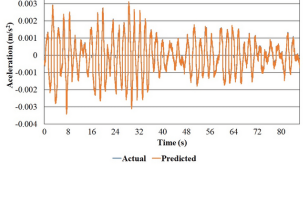
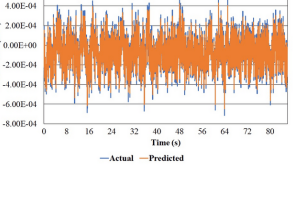
The similarity between the two gates implies that the model exhibited a parameter sharing where the flow of information through the cell is regulated and the information itself is kept in control. In addition, this supports the study conducted by De la Fuente *et al.* [22] where the model is under a temporal pattern of weight distribution, indicating that the model provides the best performance for prediction.

3.4 Model Training

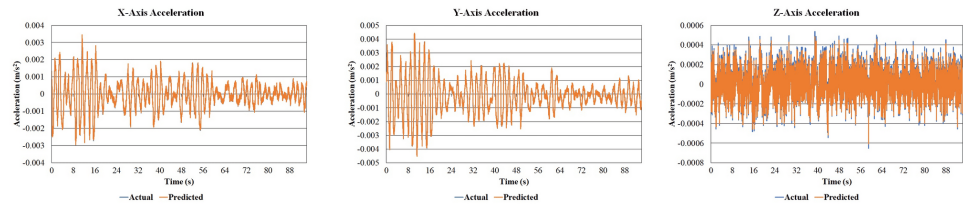
The developed RNN-LSTM model in the training sequence is used as the base data for the predicting accelerations at x, y, and z directions. In testing sequence, predictions were made using the testX sequence while testY sequence served as the actual data.

The Table 4 below presents the comparison of actual acceleration datasets for the lower, middle, and upper floors of Tower 1 and Tower 3 as well as its corresponding predicted values generated by the developed RNN-LSTM model. Moreover, it can be observed that the predicted values on the Upper (U/F) floor provided better accuracy as compared to the Lower (L/F) and Middle (M/F) floors. Although there were some slight differences on the graph between the actual and predicted values at Z-direction, the predicted values at X and Y directions have completely followed the behavior of their corresponding actual acceleration values.

Table 4 Comparison of actual and predicted acceleration data for Tower 1 and Tower 3

Building Floor	X-Direction	Y-Direction	Z-Direction
Tower 1, Lower (G/F)			
Tower 1, Middle (M/F)			
Tower 1, Upper (U/F)			
Tower 3, Lower (G/F)			
Tower 3, Middle (M/F)			

Tower 3, Upper (U/F)



Similarly, the model performance on Tower 3 presented in Table 4 shows that the U/F generated the closest replication of the actual acceleration behavior in terms of X, Y, and Z directions. Training a very large dataset allows the model to reduce the possibility of overfitting [30]. This relationship between the dataset size and prediction patterns of the model was evident, wherein the sensor acceleration data of U/F was the largest and yielded the best predictive performance in all three directions due to its large dataset size as compared to the other two floors.

3.5 Model Validation

In this study, the developed RNN-LSTM model is analyzed in terms of the number of epochs to determine the accurate hyperparameter suited for the model. Specifically, mean square error (MSE), mean absolute error (MAE), and root mean square error (RMSE) values were gathered computed for each epoch used experimentally. These metrics will also quantify the accuracy of the predicted values compared to the actual values.

Fig. 3(a) below shows the performance of the predictive data at each epoch based on mean square error (MSE). Moreover, the MSE at all floors of both towers obtained a value relative to zero. The lower the value of measured error yields to the higher accuracy of the model [31]. With the small values of MSE calculated, this signifies that there are small discrepancies between the actual and predicted values. Each floor level provides a visible difference in terms of measured error. Due to the difference in the number of recorded data, citing that higher floors are more susceptible to vibrations and tend to produce greater number of frequency data. Furthermore, it is observed that the lower the number of epochs, the higher error is recorded.

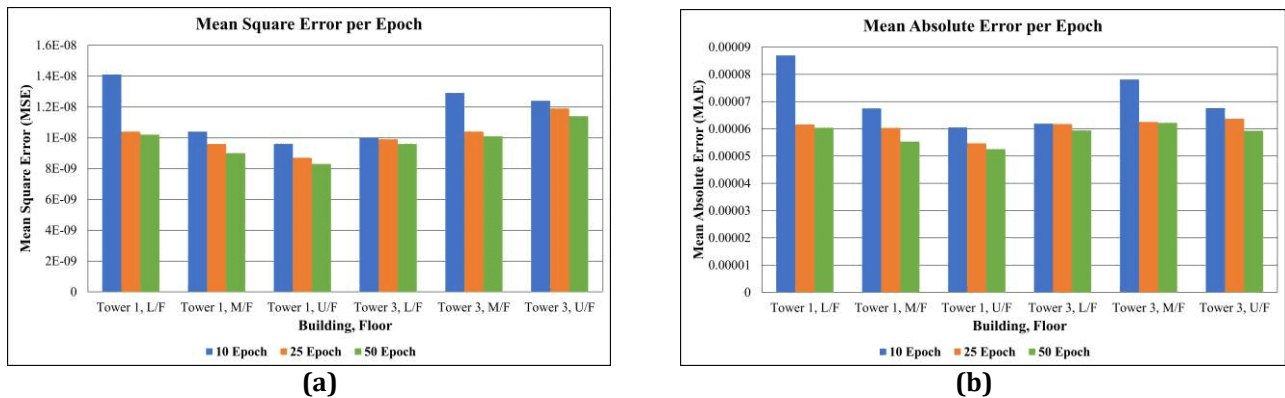


Fig. 3 (a) Mean square error (MSE); and (b) Mean absolute error (MAE) of predicted acceleration data per epoch

On the other hand, the graph in the Fig. 3(b) below presents the performance of the predicted model based on mean absolute error (MAE). Like the metric using MSE, there is a downward trend using the MAE metric in which there is a decrease on the values for each epoch. With a lower MAE, this indicates that the predictions nearly match the actual values, suggesting a better accuracy on the model [32]. In this metric, the MAE values at 50 epochs clearly displayed much lesser values. Specifically, Tower 1 U/F and Tower 3 L/F had the least values after obtaining 0.0000525622 and 0.0000594066, respectively. Therefore, it is more accurate when compared to other floor levels.

The Fig. 4 presents the root mean square error values of the predicted acceleration data at each floor. Similarly, the RMSE metric values maintained the trend observed on the previous two performance metrics, wherein the values nearly approach zero as the epoch increases. This shows that the adequacy of the RNN-LSTM model is maintained for all the metrics involved in evaluating models with large datasets similar to what was tested in this study.

The Fig. 4 presents the root mean square error values of the predicted acceleration data at each floor. Similarly, the RMSE metric values maintained the trend observed on the previous two performance metrics, wherein the values nearly approach zero as the epoch increases. This shows that the adequacy of the RNN-LSTM model is maintained for all the metrics involved in evaluating models with large datasets similar to what was tested in this study.

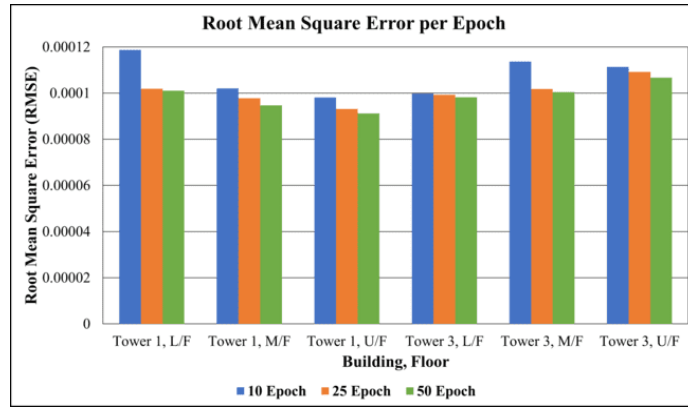


Fig. 4 Root mean square error (RMSE) of predicted acceleration data per epoch

After determining the appropriate number of epochs, the tri-axial signals of the towers used in the predictive model have been processed in terms of peak ground motion parameters, particularly peak ground acceleration (PGA), peak ground velocity (PGV), and peak ground displacement (PGD) as reported in Table 5.

Among the peak ground motion parameters, the PGA at X, Y, and Z directions of all floors had slight differences on the actual and predicted values. With regards to the values of PGA at vertical component of Tower 1, a maximum predicted value of 0.0041g has been calculated for the Y direction. Meanwhile, a maximum value of 0.0034g for the horizontal component. Although there are values obtained for the Z direction, its peak ground parameter values are relatively small as compared to the horizontal and vertical components. In terms of severity of ground shaking, the maximum predicted PGA values for both X and Y directions indicated that the tower were to experience at maximum of Intensity III. When compared back to the actual intensity felt by the building, a similar intensity PEIS scale category was recorded. This shows that the RNN-LSTM model was able to predict the extent of damage caused by ground shaking using the given hyperparameters.

Overall, this pattern in the behaviour of the performance metrics results covers the entirety of the datasets. Optimal results are obtained using 50 epochs, wherein different floor levels of both Tower 1 and Tower 3 are seen to have lower measured errors compared to other epochs. This tells that the predictive model is more accurate under 50 epochs than the other two epochs although both are already acceptable. This evidence provides an understanding that there is a significant direct relationship between the measured error and the number of epochs.

Table 5 Comparison of actual and predicted values for ground motion parameters at Tower 1

Seismic capacity parameter		PGA, g	PGV, mm/s	PGD, mm
X-Axis (L/F)	Actual	0.0023 (5.78s)	66.54 (57.30s)	1,723.00 (57.60s)
	Predicted	0.0023 (5.75s)	70.27 (57.31s)	1,835.77 (57.60s)
Y-Axis (L/F)	Actual	0.0018 (5.50s)	37.91 (56.61s)	1,100.92 (57.60s)
	Predicted	-0.0018 (5.76s)	36.14 (56.62s)	1,050.83 (57.60s)
Z-Axis (L/F)	Actual	0.0009 (3.71s)	13.68 (57.60s)	392.66 (57.60s)
	Predicted	0.0008 (3.74s)	5.99 (57.60s)	174.59 (57.60s)
X-Axis (M/F)	Actual	0.0029 (0.57s)	58.27 (91.22s)	3,062.63 (96.21s)
	Predicted	0.0030 (0.58s)	76.71 (96.21s)	3,976.27 (96.21s)
Y-Axis (M/F)	Actual	-0.0034 (19.10s)	-139.05 (93.62s)	-7,387.57 (96.21s)
	Predicted	-0.0035 (19.11s)	-135.79 (93.63s)	-7,232.07 (96.21s)

Z-Axis (M/F)	Actual	0.0006 (53.35s)	6.89 (61.70s)	397.49 (96.21s)
	Predicted	0.0006 (53.37s)	3.09 (25.49s)	75.81 (68.35s)
X-Axis (U/F)	Actual	0.0033 (14.35s)	33.58 (125.99s)	1,872.58 (129.21s)
	Predicted	0.0034 (14.38s)	20.14 (126.00s)	1,009.98 (129.21s)
Y-Axis (U/F)	Actual	-0.0041 (20.06s)	-37.13 (124.27s)	-2,708.86 (129.21s)
	Predicted	-0.0041 (20.06s)	-40.05 (129.21s)	-2,883.03 (129.21s)
Z-Axis (U/F)	Actual	0.0006 (3.42s)	56.08 (129.21s)	3,543.46 (129.21s)
	Predicted	0.0006 (3.42s)	67.41 (129.21s)	4,278.38 (129.21s)

Similarly, in Table 6, the presented data include the actual and predicted values for peak ground acceleration (PGA), peak ground velocity (PGV), and peak ground displacement (PGD) for Tower 3 using the RNN-LSTM predictive model. Regarding these parameters, the PGA had slight variations between the actual and predicted values for all floors in the X, Y, and Z directions. Specifically, the maximum predicted value for the PGA in horizontal component (X direction) is 0.0035g. As for the vertical component (Y direction), the maximum predicted value is 0.0045g. Furthermore, the maximum predicted value in Z direction is 0.0013. Considering these maximum values for PGA, the tower was predicted to experience an Intensity III categorized as moderately strong. Upon comparing the predicted intensity level based on the RNN-LSTM model with the actual intensity experienced by the building, it was observed that they both fell into the same category on the PEIS scale. This indicates that the RNN-LSTM model successfully forecasted the level of ground shaking using the provided hyperparameters.

Table 6 Comparison of actual and predicted values for ground motion parameters at Tower 3

Seismic capacity parameter		PGA, g	PGV, mm/s	PGD, mm
X-Axis (L/F)	Actual	0.0021 (21.88s)	26.52 (56.28s)	346.49 (56.28s)
	Predicted	0.0021 (21.89s)	30.14 (56.28s)	459.99 (56.28s)
Y-Axis (L/F)	Actual	-0.0024 (30.66s)	-38.46 (55.86s)	-945.68 (56.28s)
	Predicted	-0.0024 (30.67s)	-43.57 (55.86s)	-1,101.24 (56.28s)
Z-Axis (L/F)	Actual	-0.0013 (17.22s)	10.06 (51.51s)	280.35 (56.28s)
	Predicted	-0.0013 (17.22s)	10.63 (51.54s)	300.34 (56.28s)
X-Axis (M/F)	Actual	0.0025 (29.52s)	44.47 (75.32s)	1,831.44 (86.30s)
	Predicted	0.0026 (29.54s)	61.26 (75.33s)	2,657.49 (86.30s)
Y-Axis (M/F)	Actual	-0.0033 (7.46s)	-48.50 (81.70s)	-2,492.30 (86.30s)
	Predicted	-0.0034 (7.47s)	-73.64 (81.72s)	-3,636.66 (86.30s)
Z-Axis (M/F)	Actual	-0.00071 (63.92s)	-57.50 (86.30s)	-2,447.40 (86.30s)
	Predicted	-0.00064 (63.94s)	-62.44 (86.30s)	-2,662.95 (86.30s)
X-Axis (U/F)	Actual	0.0033 (11.24s)	12.73 (91.23s)	311.95 (94.22s)
	Predicted	0.0035 (11.25s)	24.34 (91.24s)	866.32 (94.22s)

Y-Axis (U/F)	Actual	-0.0045 (11.27s)	-99.76 (94.22s)	-4,735.78 (94.22s)
	Predicted	-0.0045 (11.28s)	-96.35 (94.22s)	-4,562.93 (94.22s)
Z-Axis (U/F)	Actual	-0.00065 (59.02s)	16.89 (91.89s)	637.82 (94.22s)
	Predicted	-0.00061 (59.04s)	5.49 (91.90s)	96.74 (94.22s)

4. Conclusion

The study shows the application of deep learning algorithms, particularly RNN and LSTM networks, that exhibit favourable results in constructing a predictive model to assess the seismic capacity of high-rise buildings. The main objective of the study has been successfully addressed through establishing an RNN-LSTM model for determining seismic capacity of high-rise building which yielded satisfying prediction results with minimal errors as compared to other existing methods.

The seismic data from high-rise buildings was collected from USHER Technologies Inc. and served as crucial input for the training and testing of the RNN-LSTM model. The split between the large dataset used for training and testing of the predictive model enabled it to yield values with reduced discrepancies as compared to actual values. Moreover, through defining the appropriate hyperparameters specifically seq_length and epoch, the model's performance was optimized as well as its accuracy in predicting the seismic capacity of the high-rise building.

Furthermore, the structural behaviour and performance of the high-rise building is determined through the effects of the seismic capacity parameters such as peak ground acceleration (PGA), peak ground velocity (PGV), and peak ground displacement (PGD) in the x, y, and z directions. By associating the predicted values for peak ground acceleration (PGA) and the PHIVOLCS earthquake intensity scale (PEIS), the maximum recorded intensity was determined to be Intensity III in x and y directions which indicates weak shaking on the structure. In addition, the predicted values, using response time history analysis, for the peak ground displacement (PGD) are less than 1mm. This suggests that there is minimal settlement in the structure, indicating that the ground motion did not exert a significant force. Upon comparing the predicted values to the actual values, the same conclusions can be made for the maximum intensity and peak ground displacement.

The RNN-LSTM yielded three elements in the weight lists which consists of weight matrix, recurrent weight matrix, and bias. These coefficients were used by the model to decide the output. Due to weight sharing across all time steps, the number of elements in the weights list remains consistent, wherein the established equation

for the RNN-LSTM prediction model was $o_t = (100x_t + 3h_{t-1} + 400)$. Aside from that, the accuracy of the model was evaluated using three performance metrics, namely mean square error (MSE), mean absolute error (MAE), and root mean square error (RMSE). The model yielded metrics values approaching zero, resulting in smaller discrepancies between the predicted and actual values and indicates that the RNN-LSTM has high accuracy.

Additionally, the model's performance was validated using three different methods for seismic analysis, specifically ground motion analysis, response time history analysis using the Modified- Takeda hysteresis model, and response spectrum analysis. The predicted values for the peak ground acceleration (PGA), peak ground velocity (PGV), and peak ground displacement (PGD) obtained through these analyses demonstrated small differences with the actual values, especially in the horizontal components.

The RNN-LSTM predictive model is a tool used to forecast seismic capacity of high-rise buildings based on data from accelerometer sensors. By feeding the model with a large acceleration dataset from a building, the model is trained and tested enabling it to predict acceleration values in different directions. The acceleration values obtained from the model can now be used in different methods for seismic analysis to predict the seismic capacity of the high-rise building in terms of its peak ground acceleration, peak ground velocity, and peak ground displacement.

Overall, the developed predictive model shows the use of deep learning for determining the seismic capacity of the high-rise building. This study contributes to the advancement of civil engineering methods, especially for seismic analysis by integrating data science and machine learning. The insights gained from the results will help engineers and stakeholders in making informed decisions regarding high-rise building design, retrofitting measures, and overall structural safety in relevance to seismic activities.

5. Recommendations

The objectives of the study ascertained the success of the developed RNN-LSTM model in predicting the seismic capacity of high-rise buildings. However, flaws in the approach and inadequacy in model training are determined to be the limits of the methodology. While the developed model has already displayed very high accuracy in comparison of actual and predicted values, these limits may provide an additional perspective. For

instance, values of hyperparameters seem to affect the entirety of results, it is suggested to consider distinct values with regards to sequence length, dense, and data sizes. The use of certain Keras API models is also considered crucial in model development, it is recommended to integrate other models such as functional API to determine any significant difference in accuracy when producing multiple predictions. Lastly, the study limits the type of high-rise building to Rigid Frames Structural System. It is noteworthy that differences in structural system provides different behaviours, therefore it is recommended to expand the limitations of this study to cover other building types.

Acknowledgement

This research was not funded by any grant.

Conflict of Interest

Authors declare that there is no conflict of interest regarding the publication of the paper.

Author Contribution

The authors confirm contribution to the paper as follows: **study conception and design:** Rynelle Prince A. Cabauatan, Joshua Ericson T. Dela Peña, Kirk Patrick D. Doloroso, **data collection:** Rynelle Prince A. Cabauatan, Joshua Ericson T. Dela Peña, Kirk Patrick D. Doloroso; **analysis and interpretation of results:** Rynelle Prince A. Cabauatan, Joshua Ericson T. Dela Peña, Kirk Patrick D. Doloroso, Engr. Edgardo S. Cruz, Dr. Michael B. Baylon & Dr. Francis Aldrine A. Uy; **draft manuscript preparation:** Rynelle Prince A. Cabauatan, Joshua Ericson T. Dela Peña, Kirk Patrick D. Doloroso. All authors reviewed the results and approved the final version of the manuscript.

References

- [1] Osman, A., & Malek, C. (2021) Efficient strategy for monitoring stresses in high-rise buildings, *Practice Periodical on Structural Design and Construction*, 26(4), 04021041, [https://doi.org/10.1061/\(ASCE\)SC.1943-5576.0000617](https://doi.org/10.1061/(ASCE)SC.1943-5576.0000617)
- [2] AlHamayadeh, M., & Aswad, N. G. (2022) Structural health monitoring techniques and technologies for large-scale structures: Challenges, limitations, and recommendations. *Practice Periodical on Structural Design and Construction*, 27(3), 03122004, [https://doi.org/10.1061/\(ASCE\)SC.1943-5576.0000703](https://doi.org/10.1061/(ASCE)SC.1943-5576.0000703)
- [3] Xiong, J.J., & Shenoi, R.A. (2019) General aspects on structural integrity, *Chinese Journal of Aeronautics*, 32(1), 114-132, <https://doi.org/10.1016/j.cja.2018.07.018>
- [4] Hu, R., & Xu, Y. (2019) SHM-based seismic performance assessment of high-rise buildings under long-period ground motion, *Journal of Structural Engineering*, 145(6), 04019038, [https://doi.org/10.1061/\(ASCE\)ST.1943-541X.0002323](https://doi.org/10.1061/(ASCE)ST.1943-541X.0002323)
- [5] Department of Science and Technology, Philippine Institute of Volcanology and Seismology. (2000). Distribution of active faults and liquefaction in region X. https://gisweb.phivolcs.dost.gov.ph/phivolcs_hazardmaps/11.%20Region%20X/1%20Region/Active%20Faults%20and%20Liquefaction/Active%20Faults%20and%20Liquefaction%20Map%20of%20Region%20X.pdf
- [6] Jayanthan, M., & Srinivas, V. (2015) Structural damage identification based on finite element model updating, *Journal of Mechanical Engineering and Automation*, 5(3B), 59-63, <https://doi.org/10.5923/c.jmea.201502.12>
- [7] Hussain, F., Ali, Y., & Irfan, M. (2020) An alternative approach for predicting the phase angle characteristics of asphalt concrete fixtures based on recurrent neural networks, *Journal of Materials in Civil Engineering*, 33(9), 04021215, [https://doi.org/10.1061/\(ASCE\)MT.1943-5533.0003855](https://doi.org/10.1061/(ASCE)MT.1943-5533.0003855)
- [8] Zhang, R., Chen, Z., Chen, S., Zheng, J., Büyüköztürk, O., & Sun, H. (2019) Deep long short-term memory networks for nonlinear structural seismic response prediction, *Computers and Structures*, 220, 55-68, <https://doi.org/10.1016/j.compstruc.2019.05.006>
- [9] Votsi, I., Limnios, N., Papadimitriou, E., & Tsaklidis, G. (2018) *Earthquake statistical analysis through multi-state modeling*. John Wiley & Sons, Ltd. <https://doi.org/10.1002/9781119579076>
- [10] Kagan, Y. Y. (2014). *Earthquakes: Models, statistics, testable forecasts*. John Wiley & Sons, Ltd. <https://doi.org/10.1002/9781118637913>
- [11] Velapgy, M. M., & Suresh, E. S. M. (2021). Probabilistic seismic hazard assessment model for GIS-based seismic risk study of Thiruvananthapuram City. In I. Pal, R. Shaw, R. Djalante, & S. Shrestha (Eds.), *Disaster Resilience and Sustainability* (pp. 117-149). Elsevier. <https://doi.org/10.1016/B978-0-323-85195-4.00015-9>
- [12] Wald, D. J., Jaiswal, K. S., Marano, K. D., & Bausch, D. (2011) Earthquake impact scale. *Natural Hazards Review*, 12(3), 125-139, [https://doi.org/10.1061/\(ASCE\)NH.1527-6996.0000040](https://doi.org/10.1061/(ASCE)NH.1527-6996.0000040)

- [13] Department of Public Works and Highways, Republic of the Philippines. (2019). BSDS design standard guide manual. <https://www.dpwh.gov.ph/dpwh/sites/default/files/BSDS%20Design%20Standard%20Guide%20Manual.pdf>
- [14] Peñarubia, H. C. (2019). Probabilistic seismic ground motion hazard analysis: A tool for disaster risk management [PowerPoint slides]. https://www.brainitiativesph.com/uploads/7/7/6/4/77644974/psgmha_atool4disasterriskmitigation_081919_4rsu.pdf
- [15] Luo, R., Feng, Z., Ouyang, Z., & Liu, Y. (2020) Analysis on seismic behavior of different structural systems of small high-rise buildings, *IOP Conference Series: Earth and Environmental Science*, 446, 052010, <https://doi.org/10.1088/1755-1315/446/5/052010>
- [16] Vaisakh, K.N., Nair, N. (2021). Seismic Evaluation of High Rise Buildings Using Hybrid Configuration of Grid Systems. In: Dasgupta, K., Sudheesh, T.K., Praseeda, K.I., Unni Kartha, G., Kavitha, P.E., Jawahar Saud, S. (eds) *Proceedings of SECON 2020. SECON 2020. Lecture Notes in Civil Engineering* (pp. 159-168). Springer, Cham. https://doi.org/10.1007/978-3-030-55115-5_16
- [17] Wang, C., Song, L., Yuan, Z., Fan, J. (2023) State-of-the-art AI-based computational analysis in civil engineering, *Journal of Industrial Information Integration*, 33, 100470, <https://doi.org/10.1016/j.jii.2023.100470>
- [18] Singh, E., Kuzhagaliyeva, N., & Sarathy, S. (2022). Using deep learning to diagnose preignition in turbocharged spark-ignited engines. In J. Badra, P. Pal, Y. Pei, & S. Som (Eds.), *Artificial Intelligence and Data Driven Optimization of Internal Combustion Engines* (pp. 213-237). Elsevier Inc. <https://doi.org/10.1016/B978-0-323-88457-0.00005-9>
- [19] Kim, H. (2020) Development of seismic response simulation model for building structures with semi-active control devices using recurrent neural network, *Applied Sciences*, 10(11), 3915, <https://doi.org/10.3390/app10113915>
- [20] Chen, W., Zheng, F., Gao, S., & Hu, K. (2022) An LSTM with differential structure and its application in action recognition, *Mathematical Problems in Engineering*, 2022, 7316396, <https://doi.org/10.1155/2022/7316396>
- [21] Xing, Y., Yue, J., & Chen, C. (2019) Dynamic displacement forecasting of Dashuitian Landslide in China using variational mode decomposition and stack long short-term memory network, *Applied Science*, 9(15), 2951, <https://doi.org/10.3390/app9152951>
- [22] De la Fuente, L., Ehsani, M., Gupta, H., & Condon, L. (2023). Towards Interpretable LSTM-based Modelling of Hydrological Systems. *EGU Sphere*. <https://doi.org/10.5194/egusphere-2023-666>
- [23] Hoque, K. E., & Aljamaan, H. (2021) Impact of hyperparameter tuning on machine learning models in stock price forecasting, *IEEE Access*, 9, 163815-163830, <https://doi.org/10.1109/ACCESS.2021.3134138>
- [24] Sipper, M. (2022) High Per Parameter: A Large-Scale Study of Hyperparameter Tuning for Machine Learning Algorithms, *Algorithms*, 15(9), 315, <https://doi.org/10.3390/a15090315>
- [25] Huang, Y., Han, X. & Zhao, L. (2021) Recurrent neural networks for complicated seismic dynamic response prediction of a slope system, *Engineering Geology*, 289, 106198, <https://doi.org/10.1016/j.enggeo.2021.106198>
- [26] Li, C. (2022). Machine Learning Based Seismic Structural Health Monitoring and Reconnaissance. [Doctoral dissertation, University of California, Berkeley]. UC Berkeley Electronic Theses and Dissertations. <https://escholarship.org/uc/item/39h8729w>
- [27] Arnold, T. B. (2017) KerasR: R interface to the Keras deep learning library, *Journal of Open Source Software*, 2(14), 296, <https://doi.org/10.21105/joss.00296>
- [28] Tuan, H.A. (2020) Vibration testing for dynamic properties of building floors, *IOP Conference Series: Materials Science and Engineering*, 869, 052005, <https://doi.org/10.1088/1757-899X/869/5/052005>
- [29] Toleva, B. (2021) The Proportion for Splitting Data into Training and Test Set for the Bootstrap in Classification Problems, *Business Systems Research Journal*, 12(1), 228-242, <https://doi.org/10.2478/bsri-2021-0015>
- [30] Jozefowicz, R., Vinyals, O., Schuster, M., Shazeer, N., & Wu, Y. (2016). Exploring the limits of language modeling. arXiv preprint arXiv:1602.02410. <https://doi.org/10.48550/arXiv.1602.02410>
- [31] Khatami, S. M., Naderpour, H., Razavi, S. M. N., Barros, R. C., Soltysik, B., & Jankowski, R. (2020) An ANN-based approach for prediction of sufficient seismic gap between adjacent buildings prone to earthquake-induced pounding, *Applied Sciences*, 10(10), 3591, <https://doi.org/10.3390/app10103591>
- [32] Schneider, P., & Xhafa, F. (2022). *Anomaly detection and complex event processing over IoT data streams: With application to eHealth and patient data monitoring*. Elsevier Inc. <https://doi.org/10.1016/C2020-0-00589-X>